

GraphDCA – a Framework for Node Distribution Comparison in Real and Synthetic Graphs

Ciwan Ceylan^{*12} Petra Poklukar^{*1} Hanna Hultin^{†12} Alexander Kravchenko^{†1} Anastasia Varava
Danica Kragic¹

Abstract

We argue that when comparing two graphs, the distribution of node structural features is more informative than global graph statistics which are often used in practice, especially to evaluate graph generative models. Thus, we present GraphDCA – a framework for evaluating similarity between graphs based on the alignment of their respective node representation sets. The sets are compared using a recently proposed method for comparing representation spaces, called Delaunay Component Analysis (DCA), which we extend to graph data. To evaluate our framework, we generate a benchmark dataset of graphs exhibiting different structural patterns and show, using three node structure feature extractors, that GraphDCA recognizes graphs with both similar and dissimilar local structure. We then apply our framework to evaluate three publicly available real-world graph datasets and demonstrate, using gradual edge perturbations, that GraphDCA satisfyingly captures gradually decreasing similarity, unlike global statistics. Finally, we use GraphDCA to evaluate two state-of-the-art graph generative models, NetGAN and CELL, and conclude that further improvements are needed for these models to adequately reproduce local structural features.

1. Introduction

Currently, there is no universally accepted framework for comparing graphs in terms of the distributions of their local structural properties, often referred to as node roles (Rossi & Ahmed, 2015). In particular, evaluation of graph generative models, which have potential uses in data anonymization

^{*}Equal first author contribution [†]Equal second author contribution ¹KTH Royal Institute of Technology, Stockholm, Sweden ²SEB Group, Stockholm, Sweden. Correspondence to: Ciwan Ceylan <ciwan@kth.se>, Petra Poklukar <poklukar@kth.se>.

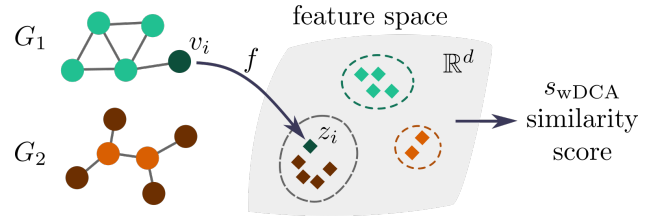


Figure 1. Overview of the GraphDCA framework which compares two input graphs, G_1 and G_2 by calculating local structural similarity score s_{wDCA} based on representations z_i corresponding to their nodes v_i obtained by a feature extractor model f .

and genetic bootstrap analysis, constitutes a difficult open problem since it is generally not possible to evaluate the quality of generated graphs using human intuition, e.g. via visual inspection as done for images (Salimans et al., 2016; Heusel et al., 2017; Sajjadi et al., 2018). To evaluate generative models for graphs, researchers have resorted to comparison of global graph statistics (Bojchevski et al., 2018; Rendsburg et al., 2020). However, as pointed out already by Bojchevski et al. (2018), global statistics are not sufficient if one is also concerned about similarity in the local structures: two locally different graphs may still have similar global properties due to the averaging across all the nodes.

Comparing node role distributions is challenging as they are typically not uniform across different roles. In particular, the presence of rare roles is common in real-world graphs and important for their analysis (Faloutsos et al., 2011; Henderson et al., 2012). For instance, in social networks there usually exist "hub" nodes with high centrality whose presence is a crucial property of the graph's topology, while only constituting a small fraction of the total number of nodes (Newman, 2018). It is therefore necessary for similarity scores between graphs to account for different role importance as defined by downstream applications.

In this work, we present the *GraphDCA* evaluation framework, visualized in Figure 1, for comparison of two graphs through the analysis of their respective node role representation sets. GraphDCA takes inspiration from the recently proposed Delaunay Component Analysis (DCA) method (Poklukar et al., 2022) which compares two sets of image

representations by analyzing the topological and geometric properties of manifolds described by the two sets. To overcome the challenge of unbalanced node role distributions and promote rare roles in the comparison analysis, we extend their scores to take into account weights of node representations.

We show that the GraphDCA framework can distinguish local structural similarities of undirected graphs without attributes when combined with a feature extractor capable of capturing such local structures. We construct a benchmark dataset of graphs, called GROLETEST, exhibiting qualitatively different connectivity patterns and thoroughly evaluate GraphDCA on it. To extract node representations, we combine GraphDCA with two state-of-the-art node role representation learning methods, GraphWave (Donnat et al., 2018) and Graph Contrastive Coding (GCC) (Qiu et al., 2020). We then apply gradual edge perturbation on three real-world graphs and demonstrate that GraphDCA favorably captures the decreasing similarity trend compared to global statistics which can exhibit large variance over different graphs and statistics. Furthermore, we employ GraphDCA to assess the quality of two recent graph generative models, NetGAN (Bojchevski et al., 2018) and CELL (Rendsburg et al., 2020), trained on both GROLETEST and real-world data and demonstrate that these models struggle to capture local structure of the training graph. Our findings suggest that improvements are necessary for these models to fully reproduce graphs’ local structural properties, in which case GraphDCA can serve as a complementary evaluation to global statistics.

2. Related Work

2.1. Graph Comparison

Traditionally, definitions of graph similarity are based on the notion of graph isomorphism such as edit distance (Sanfeliu & Fu, 1983; Gao et al., 2010) and maximum common subgraph (Bunke & Shearer, 1998). These methods are prohibitively computationally expensive and reflect how different two graphs are, e.g. how difficult it is to obtain one graph by editing another, by finding a one-to-one correspondence between nodes, which is itself a complex problem. Instead, we are interested in comparing the distributions of different node roles capturing local structural properties.

Graph kernels (Vishwanathan et al., 2010; Shervashidze et al., 2011) are typically used in graph classification tasks involving a set of graphs, often with node attributes or labels (Togninalli et al., 2019; Chen et al., 2020). Such kernels do not explicitly relate graph similarity to the distribution of local structural properties. This is unlike the modular approach of GraphDCA which measures similarity in terms of different node representations. For a recent overview of

graph kernels, see (Nikolentzos et al., 2021).

Graphlets are sometimes used in molecular applications to characterize properties of graphs and model node roles. A graphlet is a connected subgraph induced on a, usually tiny, set of nodes. Several methods for enumerating graphlets of certain size allow to characterize undirected (Hočevcar & Demšar, 2014) and directed (Sarajlić et al., 2016) graphs. The number of different graphlets grows exponentially with the number of nodes, limiting the practical size of the considered subgraphs. In addition, the set of graphlets has to be selected manually which is meaningful in applications like chemistry where graphs are *known* to be formed of certain building blocks. In contrast, we are interested in roles that do not need to be defined in advance and are *automatically* extracted from data.

2.2. Node Representations

Graph neural networks, such as (Kipf & Welling, 2017; Hamilton et al., 2017; Veličković et al., 2018; Chiang et al., 2019), excel in producing node representations for attributed graphs (Hu et al., 2020). In this work, we consider undirected graphs without attributes for which one finds two categories of node representations, capturing either neighborhood or structural similarity. The former, e.g. (Perozzi et al., 2014; Grover & Leskovec, 2016; Qiu et al., 2018), are typically learned *per graph*, and can therefore not be used in GraphDCA without modification. Instead, we focus on node representations which capture structural similarity, i.e. node roles, and can be compared across different graphs (Henderson et al., 2011; 2012; Ribeiro et al., 2017; Donnat et al., 2018; Qiu et al., 2020).

2.3. Evaluation of Generative Models for Graphs

Recently, researchers have proposed several enhancements to the general approach of comparing real and generated data in a representation space, e.g. defining precision and recall scores (Sajjadi et al., 2018; Kynkäänniemi et al., 2019) as well as comparing geometric and topological properties of the representation distributions (Khrulkov & Oseledets, 2018; Poklukar et al., 2021; 2022). In this work, we adapt the method proposed by (Poklukar et al., 2022), shown to outperform its predecessors, for comparing graphs.

Generative models for graphs are typically evaluated either by comparing global graph statistics, e.g. assortativity coefficients and motif counts, or by comparing graph descriptors consisting of a few scalar properties via Maximum Mean Discrepancy (MMD). Global statistics have been used for models trained using a single input graph (Bojchevski et al., 2018; Rendsburg et al., 2020), while MMD has been adopted in cases when several input graphs are considered (You et al., 2018; Liao et al., 2019; O’Bray et al., 2021). In this work, we are mainly concerned with comparing two large graphs

rather than two sets of smaller graphs which is why we compare with global statistics in our experiments.

3. GraphDCA Evaluation Framework

The GraphDCA evaluation framework, shown in Figure 1, compares two graphs by measuring the similarity of their local structural properties and consists of two main components:

- a *feature extractor model* f that automatically captures local structural features of the graphs as node representations, thus eliminating the need for manual feature engineering, and
- *evaluation scores* that reflect the similarity of node representation sets and can prioritize specific node roles.

To analyze the representations we extend the recently proposed Delaunay Component Analysis (DCA) (Poklukar et al., 2022) method to graphs such that the comparison can account for node role importance. We present rigorous definitions of the weighted evaluation scores in Section 3.2. GraphDCA can be combined with any feature extractor model f that maps nodes from different graphs to the same representation space. We consider two recently proposed models described in Section 3.1. Since the final choice of f depends on data and application in consideration, we additionally contribute with a synthetic dataset of graphs, called GROLETEST, exhibiting known local structures which can be used as a validation of the GraphDCA framework. We describe the generation details of GROLETEST in Section 3.3. GraphDCA inherits the hyperparameters of its two components for which we use the recommended default choices (see Appendix B.1).

3.1. Feature Extractors for Node Representations

Given two input graphs $G_k = (V_k, E_k)$ with vertex sets V_k and edge sets E_k for $k = 1, 2$, we evaluate their similarity in terms of their node representation sets $f(G_k) = \{z_i = f(v_i) \mid v_i \in V_k\}$ obtained with a feature extractor $f : V_k \rightarrow \mathbb{R}^d$. Since we are interested in representations which capture node roles in undirected graphs without node attributes, we have selected two of the latest works able to produce such representations, GraphWave (Donnat et al., 2018) and Graph Contrastive Coding (GCC) (Qiu et al., 2020). We also include a set of manually defined features for comparison.

GraphWave produces a node representation from the diffusion of a spectral graph wavelet centered at the node. Representations are constructed from these wavelets deterministically by treating them as probability distributions on the graph and characterizing the distributions using the corresponding empirical characteristic functions.

GCC uses contrastive learning to learn representations of node roles. Data instances representing a node are formed by constructing subgraphs using random-walk-based graph sampling initialized at the node. A graph neural network encodes these subgraphs into a latent space such that representations of instances originating from the same node are encoded closeby. GCC is pre-trained on a diverse set of graphs to produce general representations which can be used for downstream tasks on other graphs.

Manual features. As a baseline model f , we use manually constructed features. These are commonly used graph statistics calculated for each node’s ρ -egonet defined as the induced subgraph of all nodes within shortest path distance ρ , as previously used for $\rho = 1$ (Everett et al., 1990; Akoglu et al., 2010). Since different radii likely expose different local structures, we compute and concatenate features for $\rho \in \{1, 2, 3, 4\}$. See Appendix B.1 for the list of used statistics.

3.2. Weighted DCA Evaluation Scores

We compare two sets of node representations $R_k = f(G_k)$ for $k = 1, 2$ given by a feature extractor model f using DCA which we extend to graph data. In the original formulation of DCA, each point from R_1 and R_2 always contributes equally to the total similarity score between the two sets. While this is a reasonable assumption for the class-balanced image datasets considered by (Poklukar et al., 2022), it is problematic in the context of network analysis where distributions of different node roles are not uniform and there often exist rare roles important for the analysis. To perform the comparison of graphs based on such specific nodes roles, we extend the DCA evaluation scores to weighted representations, which we refer to as *weighted DCA*.

The idea of DCA is to compare the sets R_k by analyzing the connected components of the manifold represented by $R_1 \cup R_2$. Intuitively, if R_1 and R_2 contribute to each connected component equally and homogeneously they are considered similar. The manifold $R_1 \cup R_2$ is approximated by a so-called “distilled” Delaunay graph. First, a Delaunay graph \mathcal{D} is built to efficiently capture the neighborhood structure of the representation space. Since \mathcal{D} is always connected by construction, a clustering algorithm is applied to group the points into clusters $\{\mathcal{D}_c\}$ representing the connected components (see (Poklukar et al., 2022) for details). The obtained connected components $\{\mathcal{D}_c\}$ are then analyzed in terms of R_1 and R_2 points and edges among them expressed in several evaluation scores.

We denote by $\mathcal{H} = (\mathcal{V}, \mathcal{E})$ a *latent* graph built on a subset of representations $R_1 \cup R_2$ of given *input* graphs G_1, G_2 . Let $|\mathcal{H}|_{\mathcal{E}}$ denote the cardinality of the edge set \mathcal{E} , and let $\mathcal{H}^{R_k} = (\mathcal{V}|_{R_k}, \mathcal{E}_{R_k \times R_k})$ be the subgraph of \mathcal{H} induced by the set R_k for $k = 1, 2$. Let $w : V_1 \cup V_2 \rightarrow \mathbb{R}$ denote the weights

defined on the input graphs G_k which are further inherited to their representations R_k and consequentially to the vertex set \mathcal{V} of any latent graph \mathcal{H} , i.e., $w(\mathcal{H}) = \sum_{z_i \in \mathcal{V}} w(z_i)$.

The weighted DCA consists of three scores: *network quality* which summarizes the total geometric alignment of R_1 and R_2 across all \mathcal{D}_c , and *weighted precision and recall* which reflect the ratio of R_2 and R_1 , respectively, contained in balanced and geometrically well aligned components. These scores are derived from scores assessing the quality of each connected component \mathcal{D}_c . Intuitively, if points from R_1 and R_2 are geometrically well aligned in \mathcal{D}_c , then the ratio of latent edges between R_1 and R_2 contained in \mathcal{D}_c is high compared to the total number of latent edges. This is measured by *component quality* $q(\mathcal{D}_c) \in [0, 1]$ defined as

$$q(\mathcal{D}_c) = \begin{cases} 1 - \frac{(|\mathcal{D}_c^{R_1}|_{\varepsilon} + |\mathcal{D}_c^{R_2}|_{\varepsilon})}{|\mathcal{D}_c|_{\varepsilon}} & \text{if } |\mathcal{D}_c|_{\varepsilon} \geq 1, \\ 0 & \text{otherwise.} \end{cases}$$

The definition directly generalizes to the network quality $q(\mathcal{D})$. However, $q(\mathcal{D})$ itself does not provide insights into the position of the node representations, for example, to assess how many are contained in components of high quality. This is measured by the weighted precision $p_w \in [0, 1]$ and weighted recall $r_w \in [0, 1]$ defined as

$$p_w = \frac{\sum_{\mathcal{D}_c \in \mathcal{F}} w(\mathcal{D}_c^{R_2})}{w(\mathcal{D}^{R_2})} \quad \text{and} \quad r_w = \frac{\sum_{\mathcal{D}_c \in \mathcal{F}} w(\mathcal{D}_c^{R_1})}{w(\mathcal{D}^{R_1})},$$

where \mathcal{F} denotes the union of all high-quality \mathcal{D}_c here defined as $q(\mathcal{D}_c) > 0$. Finally, since all the scores are normalized and increasing with similarity, we define the *weighted DCA score* as their harmonic mean H

$$s_{\text{wDCA}}(R_1, R_2) = H(p_w, r_w, q). \quad (1)$$

Note that by using uniform weights, we recover the definitions given by (Poklukar et al., 2022).

3.3. GROLETTEST Synthetic Dataset

Since the choice of the feature extractor model f used in GraphDCA can be flexibly adjusted by the practitioner, we propose a dataset of synthetically generated graphs serving as a validation of the final evaluation framework. The GROLETTEST dataset (derived from *Graph "Role" Testing*) is comprised of plain, undirected and unweighted graphs having different local structures described below.

Each synthetic graph consists of a main graph m into which smaller subgraphs of a specific type h are inserted. We consider two types of main graphs: $m = \text{cycle, tree}$. The *cycle* graph consists of a single cycle, while the *tree* graph is constructed by attaching each new node to the graph with a single edge connecting it to a uniformly sampled node already contained in the graph.

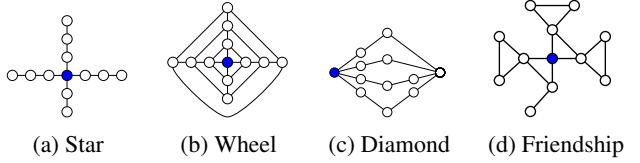


Figure 2. Subgraphs used in GROLETTEST dataset with representative central nodes (in blue).

For the subgraphs h , we consider the following five types: $h = \text{star, wheel, diamond, friendship, random}$. The first four are determined given the total number of nodes and the degree of a representative node, thought of as the central node of the subgraph. In Figure 2, we visualize an example of these subgraphs having 12 nodes and a central node of degree four (marked in blue). These are all generalizations of graphs that are typically called star, wheel, diamond and friendship in graph theory. The so-called *random* subgraphs are created by first connecting the central node with new nodes until it has the desired degree. Next, the nodes are connected uniformly at random excluding edges to the central node which keeps the desired degree. To ensure the connectivity of the subgraph, a random edge is added between each connected component and the component containing the central node, again excluding edges to the central node. Finally, each subgraph h is inserted to the main graph m by adding a predetermined number of edges between randomly chosen nodes in h and randomly chosen nodes in m .

The final GROLETTEST dataset consists of generated graphs G_h^m with a main graph m consisting of 1000 nodes and 20 instances of subgraphs h , each comprised of 40 nodes with a central node of degree 4. Each subgraph is connected to the main graph with four edges. For the *random* subgraphs, 46 random edges are sampled before all components are connected. In total, each G_h^m contains 1800 nodes.

4. Experiments

We validate GraphDCA through experiments on both GROLETTEST and three well-known real-world graphs described below. Specifically, using feature extractors f outlined in Section 3.1, we demonstrate that *i*) GraphDCA can identify GROLETTEST graphs with both similar and dissimilar distributions of local structures, and that *ii*) s_{wDCA} similarity score is robust when comparing GROLETTEST with different main graphs. Furthermore, we show that *iii*) s_{wDCA} decreases consistently with gradually perturbed graph structure both for real graphs, which we perturb globally, and GROLETTEST graphs where only known local structures are changed. Finally, we apply GraphDCA with the considered feature extractors to *iv*) evaluate two state-of-the-art generative models, NetGAN (Bojchevski et al., 2018) and CELL (Rendsburg et al., 2020), trained on both GROLETTEST and real graphs. The resulting s_{wDCA} scores suggest that these

GraphDCA Framework for Node Distribution Comparison

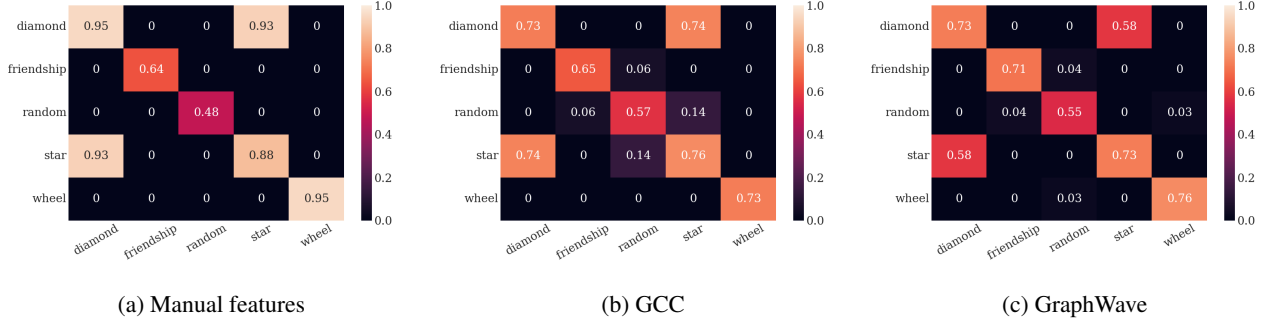


Figure 3. Matrices with values representing the average s_{wDCA} scores obtained for various feature extractors f and $G_1, G_2 \in \{G_h^{cycle} | h = \text{diamond, friendship, random, star, wheel}\}$. The scores are averaged over 3 randomly generated pairs of graphs.

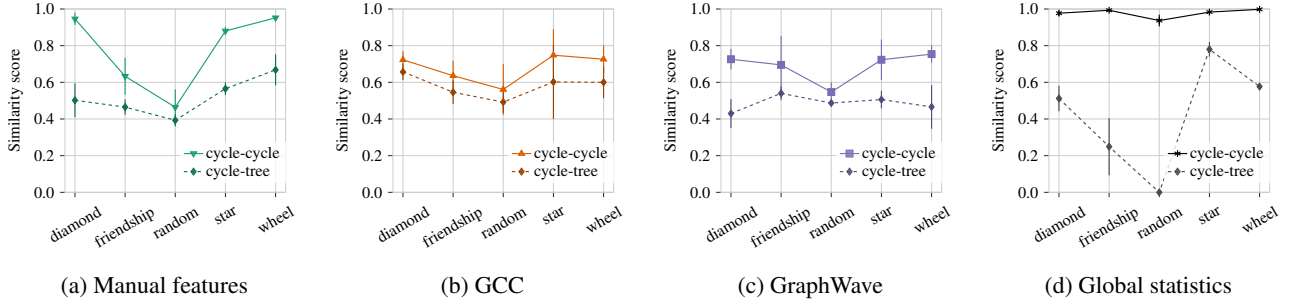


Figure 4. Average s_{wDCA} score ((a), (b), (c)) obtained between two input graphs with fixed type of subgraphs h having same main graph, i.e., $G_1 = G_h^{cycle}, G_2 = G_h^{cycle}$ (solid lines), and having different main graphs, i.e., $G_1 = G_h^{cycle}, G_2 = G_h^{tree}$ (dashed lines). The relative global statistics of input graphs $s_{gstats}(G_1, G_2)$ are shown in (d). The scores are averaged over 3 randomly generated pairs of graphs.

models struggle to capture local structure of the training graph, urging for future improvements.

Similarity scores. Since GROLETEST graphs provide ground truth information regarding node roles, we calculate s_{wDCA} with respect to the following node weights: we set $w_i = 0$ for all i except for the 20 central nodes (see Figure 2) taken as role representatives for each subgraph which we give weight $w_i = 1$. We use uniform weighting on real-world and generated graphs where roles are not specified. Results on GROLETEST obtained with uniform weights are discussed in Appendix C.

In addition to s_{wDCA} , we also compute the same global graphs statistics as in (Bojchevski et al., 2018; Rendsburg et al., 2020), i.e. maximum degree and power law exponent, the global clustering coefficient, assortativity, characteristic path length and motif counts, triangles and squares (see Table 3 in Appendix A for definitions). To facilitate comparison with s_{wDCA} , we compute the harmonic mean H of the relative difference of the individual statistics, i.e.,

$$s_{gstats}(G_1, G_2) = H \left(\left\{ 1 - \frac{|\zeta_{j,1} - \zeta_{j,2}|}{|\zeta_{j,1}| + |\zeta_{j,2}|} \right\}_j \right),$$

where $\zeta_{j,1}$ and $\zeta_{j,2}$ are the values of the same graph statistic calculated on G_1 and G_2 , respectively. Moreover, on GRO-

LETEST, we report average s_{wDCA} and s_{gstats} obtained on 3 randomly generated pairs of graphs.

Datasets. We use three well-known real-world graphs, CORA-ML, CITESEER, POLBLOGS considered in (Bojchevski et al., 2018), in addition to GROLETEST data. Each of the real-world graphs was preprocessed according to the common practice in literature: edge weights were removed, directed edges were turned into undirected, multiple edges and loops were eliminated. Finally, only the largest connected component (LCC) was used for each graph.

4.1. Local Structural Similarity

Setup. First, to verify that GraphDCA can identify similar and dissimilar local structures, we calculate $s_{wDCA}(f(G_h^{cycle}), f(G_t^{cycle}))$ for each $h, t \in \{\text{diamond, friendship, random, star, wheel}\}$ and for each of the three feature extractors f (Section 3.1). Second, to ensure that similarities are robust even when varying the global structure but preserving the local ones, we calculate similarity scores between graphs with the same subgraph types but different main graphs, $s_{wDCA}(f(G_h^{cycle}), f(G_h^{tree}))$.

Results and discussion. We report the average s_{wDCA} scores in the form of matrices in Figure 3. Firstly, we observe that the scores obtained with all f are prevailing

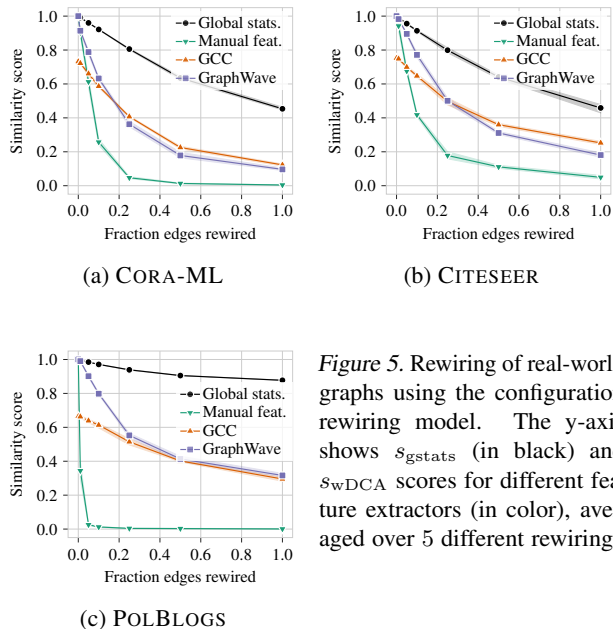


Figure 5. Rewiring of real-world graphs using the configuration rewiring model. The y-axis shows s_{gstats} (in black) and s_{wDCA} scores for different feature extractors (in color), averaged over 5 different rewirings.

on the diagonal which is the desired behavior. Secondly, all models detect similarity between $G_{diamond}^{cycle}$ and G_{star}^{cycle} and a lower similarity score between G_{random}^{cycle} graphs. The similarity between *diamond* and *star* subgraphs is expected as the only difference between these subgraphs are 3 additional edges in the *diamond* which are all far away from the central node. These additional edges are not included in the manual features as these only consider nodes within shortest path distance of 4. Similarly, it is highly unlikely for GCC to include these edges due to the restart probability of the random walks. Consequently, GraphWave is the only feature extractor yielding noticeably lower scores between *diamond* and *star* than between *diamond* and *diamond*. The lower similarity score between *random* subgraphs is also expected since these subgraphs, unlike the other subgraph types, are only similar and not identical. Due to their random structure, G_{random}^{cycle} are in some cases slightly similar to other subgraphs (Figure 3b).

In Figure 4, we show s_{wDCA} for graph pairs $(G_h^{cycle}, G_h^{tree})$ having similar local h but different global structure m (dashed lines), and graph pairs $(G_h^{cycle}, G_h^{cycle})$ with both similar local and global structure (solid lines). We observe that global statistics similarity s_{gstats} (Figure 4d) varies significantly across different input combinations. For example, s_{gstats} changes drastically for *random* subgraphs, exhibits large variance for *friendship* and only changes slightly for *star* subgraphs. On the other hand, s_{wDCA} scores are largely robust to changes in the main graph, especially for representations obtained with GCC (Figure 4b). The s_{wDCA} scores do change more when using manual features (Figure 4a) possibly since these are more sensitive to minor changes in the graph given that single edges can significantly change the ρ -egonet structure.

4.2. Gradual Structure Perturbation

To show that s_{wDCA} can capture gradually decreasing similarity, we preform structure perturbation experiments on the three real-world graphs and the GROLETEST graphs.

Setup. For the real-world graphs, we use the configuration rewiring model where edges are rewired such that the degree distributions of the graphs remain unchanged but not local structures. For GROLETEST, we only perturb the subgraph structures. Instead of configuration rewiring, we first find a random minimum spanning tree of the subgraph, randomly remove edges from the subgraph not present in the tree, and add random previously non-existing edges in the subgraph. In both cases, we measure the perturbation as the fraction of rewired, added or removed edges to the number of edges in the original graph. We report the similarity scores averaged over 5 different rewirings per fraction. See Appendix B.2 for additional details on the perturbation procedure.

Results and discussion. In Figure 5, we visualize the scores obtained on real-world graphs. We observe that s_{wDCA} with all f and s_{gstats} drop consistently as the edges are rewired. The changes in global statistics are mainly attributed to changes in the global clustering coefficient and number of triangle/squares which may differ by up to a factor 7 between the original and rewired graphs. Since configuration rewiring is used, max degree and power law exponent are unaffected, while we observe that the assortativity and characteristic path length change at most by a factor of 2. For POLBLOGS, s_{gstats} remains high even after all edges have been rewired since this graph is much denser than the two citation graphs, CORA-ML and CITESEER, with average degree 27 compared to 5.6 and 3.5, respectively. Consequently, the global clustering coefficient and motif counts do not drop as much during rewiring of POLBLOGS since new triangles and squares are more likely to form during the rewiring.

While the behavior of the GraphWave and GCC representations is consistent across all datasets, s_{wDCA} obtained with manual features drops rapidly for POLBLOGS. We conjecture the cause to be the presence of two distinct communities, corresponding to the two major US political parties (Adamic & Glance, 2005). Rewiring of single edges may result in significant changes in the ρ -egonet structure as community bridges are formed or broken. This in turn induces larger changes in the distribution of the manual features compared to the GraphWave and GCC which are not as sensitive to single edge perturbations. A final observation is that s_{wDCA} obtained with GCC never reaches 1.0 even when two isomorphic graphs are compared which is expected as GCC feature extraction is not deterministic.

The similarity scores obtained on GROLETEST are shown in Figure 6. We observe a largely consistent gradual drop of

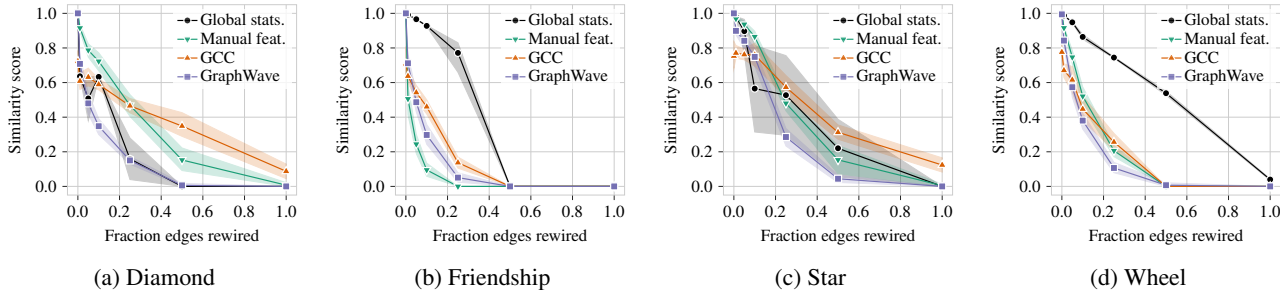


Figure 6. Rewiring of GROLETEST subgraphs via the addition and removal of edges. The x-axis specifies the fraction of changed edges. The y-axis shows s_{gstats} scores (in black) and s_{wDCA} scores for different feature extractors (in color), averaged over 5 different rewirings.

s_{wDCA} obtained using different feature extractors f , where GraphWave representations exhibit particularly low variance. On the contrary, the behavior of s_{gstats} differs significantly between the subgraph types as edge perturbation affects the global statistics differently depending on the subgraph structure. For the *diamond* and *star* subgraphs, the characteristic path length changes consistently with the perturbation, while the power law exponential drops from 20.7 to 2.4 with just 1% of perturbed edges. This sudden change is not observed for *friendship* and *wheel* which instead exhibit larger changes in assortativity, global clustering coefficient and number of triangles. This highlights the stability of s_{wDCA} compared to the sensitivity of the choice of global statistics.

4.3. Evaluation of Graph Generative Models

We demonstrate how GraphDCA can provide valuable insights for evaluation of graph generative models which is an important open problem. We consider the recently proposed NetGAN and CELL generative models trained on both GROLETEST and real-world datasets. Comparing these models is particularly interesting as CELL is essentially a NetGAN model stripped of the GAN component, while arguably retaining its performance.

Setup. Prior to the training of the models, the edges of each preprocessed graph were split into 85% train, 10% validation and 5% test sets, following the procedure from (Bojchevski et al., 2018). NetGAN was separately trained with 50% edge overlap (EO) and link prediction validation (Val) stopping criteria. CELL model was trained using the same splits with 50% EO criterion. Hyperparameters and experimental details on training and generation can be found in Appendix B.3. We run GraphDCA on three randomly generated graphs G_2 for each considered training graph G_1 .

Results and discussion. The s_{wDCA} scores and global statistics obtained on real-world graphs are shown in Table 1. Both NetGAN and CELL capture most of the global properties well which is expected since global statistics likely served as a methodological validation during the model development. However, they struggle to reproduce triangles

and squares – local statistics that is often overlooked despite consistently being non reproducible (Rendsburg et al., 2020). With such large differences in triangle and square counts (often over 50%), evaluation of the preservation of local structures in the generated graphs is challenging.

On the other hand, s_{wDCA} with different feature extractors exhibit similar ratios as in the rewiring experiments in Section 4.2. Interestingly, the scores obtained for all three types of graphs are close to the values observed after the rewiring of $\sim 20\%$ edges (see Figure 5). Since approximately 50% of the edges are different in the generated and the training graphs, this indicates a certain degree of generalization achieved by the models and confirms that model performance is not defined by high edge overlap criterion.

When comparing the performance of two models via s_{wDCA} , the ratio between NetGAN and CELL scores is consistent across different f . For CORA-ML and CITESEER, this ratio is ~ 1.2 , indicating that NetGAN outperforms CELL to a small extent. The similarity between the scores for the two datasets can be due to the semantic similarity of the graphs which are both citation networks. In contrast, CELL outperforms NetGAN on POLBLOGS (with score ratio ~ 0.75), possibly due to a larger density of the graph which might be more sensitive to the number of random walks sampled in NetGAN. Overall, both models produce medium s_{wDCA} scores on the real-world graphs indicating poor reproducibility of the local patterns. The bias towards reproduction of global statistics is particularly visible in s_{wDCA} obtained with the manual features which are more sensitive to changes in the local structure.

In Table 2 we report the results obtained on GROLETEST for $h = diamond, friendship, wheel$ (for $h = random, star$ see Table 5 in Appendix C.3). We observe that the models struggle to produce graphs that would well reflect all the global statistics. This is possibly due to a combination of low density of the graphs (average degree is not higher than 2) and high characteristic path length (ca. 40-80). Short random walks utilized by NetGAN and low-rank logit space in CELL have lower capability of capturing the sparsity of the graph as models have to store progressively more informa-

GraphDCA Framework for Node Distribution Comparison

Table 1. Global graph statistics of the real-world training graphs G_1 and s_{wDCA} scores obtained on representations extracted from the considered feature extractors f of G_1 and graphs G_2 generated by NetGAN and CELL (50% EO stopping criterion). The scores are averaged over 3 independently generated graphs with the same training split.

	CORA-ML			CITISEER			POLBLOGS		
	GROUND TRUTH	NETGAN	CELL	GROUND TRUTH	NETGAN	CELL	GROUND TRUTH	NETGAN	CELL
MAX DEGREE	238	216.00 ± 11.14	191.33 ± 6.51	76	88.00 ± 1.73	67 ± 1.73	303	279.33 ± 14.57	250.00 ± 6.24
ASSORTATIVITY	-0.08	-0.08 ± 0.00	-0.07 ± 0.00	-0.19	-0.16 ± 0.00	-0.2 ± 0.01	-0.22	-0.25 ± 0.01	-0.25 ± 0.00
TRIANGLE COUNT	2,802	1,772.33 ± 17.39	1,409.67 ± 50.85	304	195.33 ± 5.86	88.33 ± 10.69	61,108	36,294.33 ± 348.62	44,862.33 ± 275.61
SQUARE COUNT	14,268	6,741.33 ± 229.38	7,035.00 ± 424.89	1,441	371.33 ± 35.22	420.33 ± 16.26	2,654,319	1,350,075.67 ± 17073.43	1,801,022.33 ± 7383.63
POWER LAW EXP.	1.86	1.81 ± 0.00	1.82 ± 0.00	2.45	2.32 ± 0.01	2.39 ± 0.00	1.44	1.41 ± 0.00	1.43 ± 0.00
CLUSTERING COEFF.	0.08	0.06 ± 0.00	0.05 ± 0.00	0.04	0.03 ± 0.00	0.02 ± 0.00	0.19	0.13 ± 0.00	0.15 ± 0.00
CHARC. PATH LEN.	5.63	5.23 ± 0.03	5.24 ± 0.05	8.02	6.49 ± 0.20	6.33 ± 0.04	2.82	2.67 ± 0.00	2.77 ± 0.01
s_{wDCA} - MANUAL	1.00	0.11 ± 0.01	0.08 ± 0.00	1.00	0.22 ± 0.01	0.17 ± 0.03	1.00	0.00 ± 0.00	0.00 ± 0.00
s_{wDCA} - GCC	0.73	0.51 ± 0.00	0.43 ± 0.00	0.75	0.50 ± 0.01	0.44 ± 0.01	0.66	0.38 ± 0.02	0.48 ± 0.04
s_{wDCA} - GRAPHWAVE	1.00	0.52 ± 0.01	0.46 ± 0.02	1.00	0.53 ± 0.03	0.50 ± 0.02	1.00	0.50 ± 0.01	0.70 ± 0.01

Table 2. Global graph statistics of GROLETEST training graphs G_1 and s_{wDCA} scores obtained on representations extracted from the considered feature extractors f of G_1 and graphs G_2 generated by NetGAN and CELL (50% EO stopping criterion). The scores are averaged over 3 independently generated graphs with the same training split.

	DIAMOND			FRIENDSHIP			WHEEL		
	GROUND TRUTH	NETGAN	CELL	GROUND TRUTH	NETGAN	CELL	GROUND TRUTH	NETGAN	CELL
MAX DEGREE	5	6.33 ± 0.58	7.00 ± 1.00	6	6.67 ± 0.58	7.0 ± 0.00	6	8.00 ± 0.00	8.00 ± 1.00
ASSORTATIVITY	0.05	-0.10 ± 0.03	0.08 ± 0.02	0.19	-0.10 ± 0.01	0.08 ± 0.02	0.46	-0.00 ± 0.00	0.14 ± 0.01
TRIANGLE COUNT	0	116.67 ± 3.79	0.00 ± 0.00	100	123.00 ± 3.00	34.67 ± 6.11	47	251.33 ± 13.01	17.33 ± 0.58
SQUARE COUNT	0	51.0 ± 9.85	14.00 ± 5.57	0	65.00 ± 6.24	24.67 ± 4.04	284	192.67 ± 2.08	127.33 ± 11.24
POWER LAW EXP.	2.51	2.72 ± 0.01	2.66 ± 0.01	2.45	2.59 ± 0.00	2.56 ± 0.01	2.16	2.25 ± 0.01	2.23 ± 0.00
CLUSTERING COEFF.	0.00	0.14 ± 0.01	0.00 ± 0.00	0.11	0.12 ± 0.00	0.03 ± 0.01	0.04	0.16 ± 0.01	0.01 ± 0.00
CHARC. PATH LEN.	82.72	11.71 ± 1.28	19.60 ± 0.91	51.44	27.77 ± 0.32	15.56 ± 0.26	39.85	19.44 ± 3.33	11.25 ± 0.06
s_{wDCA} - MANUAL	1.00 ± 0.00	0.37 ± 0.04	0.68 ± 0.04	1.00 ± 0.00	0.45 ± 0.02	0.48 ± 0.01	1.00 ± 0.00	0.22 ± 0.06	0.29 ± 0.01
s_{wDCA} - GCC	0.80 ± 0.01	0.38 ± 0.01	0.64 ± 0.03	0.77 ± 0.00	0.52 ± 0.01	0.57 ± 0.01	0.70 ± 0.02	0.34 ± 0.01	0.42 ± 0.01
s_{wDCA} - GRAPHWAVE	1.00 ± 0.00	0.17 ± 0.02	0.34 ± 0.01	1.00 ± 0.00	0.31 ± 0.02	0.39 ± 0.03	1.00 ± 0.00	0.22 ± 0.01	0.20 ± 0.01

tion about the local structure to avoid shortcuts. Moreover, we observe that global statistics exhibit larger variations across different generated graphs of the same type than in real-world graphs. In contrast, s_{wDCA} values still have low variation compared to the unstable global statistics, and higher confidence in the model evaluation. Across all 5 subgraph types, CELL outperforms NetGAN in terms of s_{wDCA} scores, indicating its higher ability in capturing the local structure of low-density graphs. This effect can also be illustrated by the fact that CELL produces graphs with 0 triangle count when trained on graphs without triangles (*diamond*, *star*, *random*), while NetGAN pollutes local properties of the nodes. The CELL s_{wDCA} scores obtained with manual features are accordingly relatively high for these graphs. The overall low s_{wDCA} scores show that neither NetGAN nor CELL can generate graphs that resemble well the training graphs, although CELL is more efficient in replicating the egocentric networks in GROLETEST graphs.

Finally, we compare graphs generated by NetGAN models trained with EO and Val stopping criteria. The global statistics and s_{wDCA} scores can be found in Table 4 in Appendix C.3. The results support previous conclusions about higher efficiency of the edge overlap criterion in generating new graphs. It is worth noting that in cases when all global statistics are either both similar or both different from the

training values (e.g., on CORA-ML), s_{wDCA} scores provide a more clear comparison between two models, in this case in favor of EO criterion.

5. Conclusion

We establish GraphDCA as a graph similarity evaluation framework able to compensate the deficiencies of global statistics by instead comparing graphs in terms of their local structural properties. Using three different feature extractors producing node role representations, GraphDCA is able to recognize graphs with similar subgraph structures and differentiate between graphs not sharing such similarities. We showed how GraphDCA can be applied to evaluate generative models for graphs and concluded that while current state-of-the-art models are able to capture many global statistics of training graphs, improvements for reproducing local structures are needed. A natural next step is to use the insights provided by GraphDCA to further develop and enhance generative models for graphs with this capability. Though GraphDCA can be applied to any graphs given suitable feature extractors, we have in this work focused on plain, undirected and unweighted graphs and leave evaluation using attributed, directed and/or weighted graphs to future work.

Acknowledgements

This work has been supported by the Knut and Alice Wallenberg Foundation, Swedish Research Council and European Research Council. The authors thank Vladislav Polianskii, Miguel Vasco, Kambiz Ghoorchian and Ala Tarighati for their valuable suggestions and feedback.

References

- Adamic, L. A. and Glance, N. The political blogosphere and the 2004 u.s. election: Divided they blog. In *Proceedings of the 3rd International Workshop on Link Discovery*, LinkKDD '05, pp. 36–43, New York, NY, USA, 2005. Association for Computing Machinery. ISBN 1595932151. doi: 10.1145/1134271.1134277. URL <https://doi.org/10.1145/1134271.1134277>.
- Akoglu, L., McGlohon, M., and Faloutsos, C. oddball: Spotting Anomalies in Weighted Graphs. In *PAKDD*, 2010. doi: 10.1007/978-3-642-13672-6_40.
- Bojchevski, A., Shchur, O., Zügner, D., and Günnemann, S. NetGAN: Generating Graphs via Random Walks. In *International Conference on Machine Learning*, pp. 610–619. PMLR, July 2018. URL <http://proceedings.mlr.press/v80/bojchevski18a.html>. ISSN: 2640-3498.
- Bunke, H. and Shearer, K. A graph distance metric based on the maximal common subgraph. *Pattern Recognition Letters*, 19(3):255–259, 1998. ISSN 0167-8655. doi: [https://doi.org/10.1016/S0167-8655\(97\)00179-7](https://doi.org/10.1016/S0167-8655(97)00179-7). URL <https://www.sciencedirect.com/science/article/pii/S0167865597001797>.
- Chen, D., Jacob, L., and Mairal, J. Convolutional kernel networks for graph-structured data. In *International Conference on Machine Learning*, pp. 1576–1586. PMLR, 2020.
- Chiang, W.-L., Liu, X., Si, S., Li, Y., Bengio, S., and Hsieh, C.-J. Cluster-gcn: An efficient algorithm for training deep and large graph convolutional networks. In *Proceedings of the 25th ACM SIGKDD International Conference on Knowledge Discovery & Data Mining*, pp. 257–266, 2019.
- Donnat, C., Zitnik, M., Hallac, D., and Leskovec, J. Learning Structural Node Embeddings Via Diffusion Wavelets. In *Proceedings of the 24th ACM SIGKDD International Conference on Knowledge Discovery & Data Mining*, KDD'18, pp. 1320–1329, New York, NY, USA, July 2018. Association for Computing Machinery. doi: 10.1145/3219819.3220025. URL <http://arxiv.org/abs/1710.10321>. arXiv: 1710.10321.
- Everett, M. G., Boyd, J. P., and Borgatti, S. P. Ego-centered and local roles: A graph theoretic approach. *Journal of Mathematical Sociology*, 15(3-4):163–172, 1990.
- Faloutsos, M., Faloutsos, P., and Faloutsos, C. *On power-law relationships of the internet topology*, pp. 195–206. Princeton University Press, 2011. doi: 10.1515/9781400841356.195. URL <https://doi.org/10.1515/9781400841356.195>.
- Gao, X., Xiao, B., Tao, D., and Li, X. A survey of graph edit distance. *Pattern Analysis and applications*, 13(1): 113–129, 2010.
- Grover, A. and Leskovec, J. node2vec: Scalable Feature Learning for Networks. In *Proceedings of the 22nd ACM SIGKDD International Conference on Knowledge Discovery and Data Mining - KDD '16*, pp. 855–864, San Francisco, California, USA, 2016. ACM Press. ISBN 978-1-4503-4232-2. doi: 10.1145/2939672.2939754. URL <http://dl.acm.org/citation.cfm?doid=2939672.2939754>.
- Hamilton, W., Ying, Z., and Leskovec, J. Inductive representation learning on large graphs. In Guyon, I., Luxburg, U. V., Bengio, S., Wallach, H., Fergus, R., Vishwanathan, S., and Garnett, R. (eds.), *Advances in Neural Information Processing Systems*, volume 30. Curran Associates, Inc., 2017. URL <https://proceedings.neurips.cc/paper/2017/file/5dd9db5e033da9c6fb5ba83c7a7e9bea9-Paper.pdf>.
- Henderson, K., Gallagher, B., Li, L., Akoglu, L., Eliassi-Rad, T., Tong, H., and Faloutsos, C. It's who you know: graph mining using recursive structural features. In *Proceedings of the 17th ACM SIGKDD international conference on Knowledge discovery and data mining*, KDD '11, pp. 663–671, New York, NY, USA, August 2011. Association for Computing Machinery. ISBN 978-1-4503-0813-7. doi: 10.1145/2020408.2020512. URL <https://doi.org/10.1145/2020408.2020512>.
- Henderson, K., Gallagher, B., Eliassi-Rad, T., Tong, H., Basu, S., Akoglu, L., Koutra, D., Faloutsos, C., and Li, L. RolX: structural role extraction & mining in large graphs. In *Proceedings of the 18th ACM SIGKDD international conference on Knowledge discovery and data mining*, KDD '12, pp. 1231–1239, New York, NY, USA, August 2012. Association for Computing Machinery. ISBN 978-1-4503-1462-6. doi: 10.1145/2339530.2339723. URL <https://doi.org/10.1145/2339530.2339723>.
- Heusel, M., Ramsauer, H., Unterthiner, T., Nessler, B., and Hochreiter, S. Gans trained by a two time-scale update rule converge to a local nash equilibrium. In Guyon, I.,

- Luxburg, U. V., Bengio, S., Wallach, H., Fergus, R., Vishwanathan, S., and Garnett, R. (eds.), *Advances in Neural Information Processing Systems*, volume 30. Curran Associates, Inc., 2017. URL <https://proceedings.neurips.cc/paper/2017/file/8a1d694707eb0fefe65871369074926d-Paper.pdf>.
- Hočevar, T. and Demšar, J. A combinatorial approach to graphlet counting. *Bioinformatics*, 30(4): 559–565, 12 2014. ISSN 1367-4803. doi: 10.1093/bioinformatics/btt717. URL <https://doi.org/10.1093/bioinformatics/btt717>.
- Hu, W., Fey, M., Zitnik, M., Dong, Y., Ren, H., Liu, B., Catasta, M., and Leskovec, J. Open graph benchmark: Datasets for machine learning on graphs. *arXiv preprint arXiv:2005.00687*, 2020.
- Khrulkov, V. and Oseledets, I. Geometry score: A method for comparing generative adversarial networks. In *International Conference on Machine Learning*, pp. 2621–2629. PMLR, 2018.
- Kipf, T. N. and Welling, M. Semi-supervised classification with graph convolutional networks. In *5th International Conference on Learning Representations, ICLR 2017, Toulon, France, April 24-26, 2017, Conference Track Proceedings*. OpenReview.net, 2017. URL <https://openreview.net/forum?id=SJU4ayYgl>.
- Kynkäänniemi, T., Karras, T., Laine, S., Lehtinen, J., and Aila, T. Improved precision and recall metric for assessing generative models. In Wallach, H., Larochelle, H., Beygelzimer, A., d'Alché-Buc, F., Fox, E., and Garnett, R. (eds.), *Advances in Neural Information Processing Systems*, volume 32. Curran Associates, Inc., 2019. URL <https://proceedings.neurips.cc/paper/2019/file/0234c510bc6d908b28c70ff313743079-Paper.pdf>.
- Liao, R., Li, Y., Song, Y., Wang, S., Hamilton, W., Duvenaud, D. K., Urtasun, R., and Zemel, R. Efficient graph generation with graph recurrent attention networks. In Wallach, H., Larochelle, H., Beygelzimer, A., d'Alché-Buc, F., Fox, E., and Garnett, R. (eds.), *Advances in Neural Information Processing Systems*, volume 32. Curran Associates, Inc., 2019. URL <https://proceedings.neurips.cc/paper/2019/file/d0921d442ee91b896ad95059d13df618-Paper.pdf>.
- Newman, M. *Networks*. Oxford university press, 2nd edition, 2018. ISBN 978-0-19-880509-0. doi: <https://doi.org/10.1093/oso/9780198805090.001.0001>.
- Newman, M. E. The structure and function of complex networks. *SIAM review*, 45(2):167–256, 2003a.
- Newman, M. E. J. Mixing patterns in networks. *Phys. Rev. E*, 67:026126, Feb 2003b. doi: 10.1103/PhysRevE.67.026126. URL <https://link.aps.org/doi/10.1103/PhysRevE.67.026126>.
- Nikolentzos, G., Siglidis, G., and Vazirgiannis, M. Graph kernels: A survey. *Journal of Artificial Intelligence Research*, 72:943–1027, 2021.
- O’Bray, L., Horn, M., Rieck, B., and Borgwardt, K. Evaluation metrics for graph generative models: Problems, pitfalls, and practical solutions, 2021.
- Perozzi, B., Al-Rfou, R., and Skiena, S. DeepWalk: online learning of social representations. In *Proceedings of the 20th ACM SIGKDD international conference on Knowledge discovery and data mining, KDD ’14*, pp. 701–710, New York, NY, USA, August 2014. Association for Computing Machinery. ISBN 978-1-4503-2956-9. doi: 10.1145/2623330.2623732. URL <https://doi.org/10.1145/2623330.2623732>.
- Poklukar, P., Varava, A., and Kragic, D. Geomca: Geometric evaluation of data representations. In Meila, M. and Zhang, T. (eds.), *Proceedings of the 38th International Conference on Machine Learning Research*, pp. 8588–8598. PMLR, 18–24 Jul 2021. URL <https://proceedings.mlr.press/v139/poklukar21a.html>.
- Poklukar, P., Polianskii, V., Varava, A., Pokornyy, F. T., and Jensfelt, D. K. Delaunay component analysis for evaluation of data representations. In *International Conference on Learning Representations*, 2022. URL <https://openreview.net/forum?id=HTVch9AMPa>.
- Qiu, J., Dong, Y., Ma, H., Li, J., Wang, K., and Tang, J. Network Embedding as Matrix Factorization: Unifying DeepWalk, LINE, PTE, and Node2vec. In *Proceedings of the eleventh ACM international conference on web search and data mining, WSDM ’18*, pp. 459–467, New York, NY, USA, 2018. Association for Computing Machinery. ISBN 978-1-4503-5581-0. doi: 10.1145/3159652.3159706. URL <https://doi.org/10.1145/3159652.3159706>. event-place: Marina Del Rey, CA, USA.
- Qiu, J., Chen, Q., Dong, Y., Zhang, J., Yang, H., Ding, M., Wang, K., and Tang, J. GCC: Graph Contrastive Coding for Graph Neural Network Pre-Training. In *Proceedings of the 26th ACM SIGKDD International Conference on Knowledge Discovery & Data Mining, KDD’20*, pp. 1150–1160. Association for Computing Machinery, New

- York, NY, USA, August 2020. ISBN 978-1-4503-7998-4. URL <https://doi.org/10.1145/3394486.3403168>.
- Rendsburg, L., Heidrich, H., and Luxburg, U. V. NetGAN without GAN: From Random Walks to Low-Rank Approximations. In III, H. D. and Singh, A. (eds.), *Proceedings of the 37th International Conference on Machine Learning*, volume 119 of *Proceedings of Machine Learning Research*, pp. 8073–8082. PMLR, July 2020. URL <http://proceedings.mlr.press/v119/rendersburg20a.html>.
- Ribeiro, L. F., Saverese, P. H., and Figueiredo, D. R. struc2vec: Learning node representations from structural identity. In *Proceedings of the 23rd ACM SIGKDD international conference on knowledge discovery and data mining*, pp. 385–394, 2017.
- Rossi, R. A. and Ahmed, N. K. Role Discovery in Networks. *IEEE Transactions on Knowledge and Data Engineering*, 27(4):1112–1131, April 2015. ISSN 1558-2191. doi: 10.1109/TKDE.2014.2349913. Conference Name: IEEE Transactions on Knowledge and Data Engineering.
- Sajjadi, M. S. M., Bachem, O., Lucic, M., Bousquet, O., and Gelly, S. Assessing generative models via precision and recall. In Bengio, S., Wallach, H., Larochelle, H., Grauman, K., Cesa-Bianchi, N., and Garnett, R. (eds.), *Advances in Neural Information Processing Systems*, volume 31. Curran Associates, Inc., 2018. URL <https://proceedings.neurips.cc/paper/2018/file/f7696a9b362ac5a51c3dc8f098b73923-Paper.pdf>.
- Salimans, T., Goodfellow, I., Zaremba, W., Cheung, V., Radford, A., and Chen, X. Improved techniques for training gans. *Advances in neural information processing systems*, 29:2234–2242, 2016.
- Sanfeliu, A. and Fu, K.-S. A distance measure between attributed relational graphs for pattern recognition. *IEEE Transactions on Systems, Man, and Cybernetics*, SMC-13(3):353–362, 1983. doi: 10.1109/TSMC.1983.6313167.
- Sarajlić, A., Malod-Dognin, N., Yaveroğlu, Ö. N., and Pržulj, N. Graphlet-based characterization of directed networks. *Scientific reports*, 6(1):1–14, 2016.
- Shervashidze, N., Schweitzer, P., Van Leeuwen, E. J., Mehlhorn, K., and Borgwardt, K. M. Weisfeiler-lehman graph kernels. *Journal of Machine Learning Research*, 12(9), 2011. URL <https://www.jmlr.org/papers/volume12/shervashidze11a/shervashidze11a.pdf>.
- Togninalli, M., Ghisu, E., Llinares-López, F., Rieck, B., and Borgwardt, K. Wasserstein weisfeiler-lehman graph kernels. In Wallach, H., Larochelle, H., Beygelzimer, A., d'Alché-Buc, F., Fox, E., and Garnett, R. (eds.), *Advances in Neural Information Processing Systems*, volume 32. Curran Associates, Inc., 2019. URL <https://proceedings.neurips.cc/paper/2019/file/73fed7fd472e502d8908794430511f4d-Paper.pdf>.
- Veličković, P., Cucurull, G., Casanova, A., Romero, A., Liò, P., and Bengio, Y. Graph Attention Networks. *International Conference on Learning Representations*, 2018. URL <https://openreview.net/forum?id=rJXMpikCZ>.
- Vishwanathan, S. V. N., Schraudolph, N. N., Kondor, R., and Borgwardt, K. M. Graph kernels. *Journal of Machine Learning Research*, 11:1201–1242, 2010. URL <https://www.jmlr.org/papers/volume11/vishwanathan10a/vishwanathan10a.pdf>.
- You, J., Ying, R., Ren, X., Hamilton, W., and Leskovec, J. Graphrnn: Generating realistic graphs with deep autoregressive models. In *International Conference on Machine Learning*, pp. 5708–5717. PMLR, 2018.

A. Graph Statistics

We provide the exact definitions of global graph statistics used in our experiments in Table 3.

B. Additional Details

B.1. GraphDCA Hyperparameters

The GraphDCA framework naturally inherits hyperparameters of the chosen feature extractor model f and hyperparameters associated to the Delaunay graph approximation performed in DCA (Poklukar et al., 2022). Originally, DCA has four hyperparameters: T affecting the number of found Delaunay edges, B used as an optional parameter for reducing the number of Delaunay edges, and mcs determining the number of points needed to form a cluster. In our experiments, we use default options for $T = 10,000$ and $B = 1.0$, and set $mcs = 2$.

Similarly, we used the default hyperparameters for GraphWave, namely: $d = 50$ (i.e. 25 sample points of the empirical characteristic function), order 30 Chebyshev polynomials and two filter values t selected automatically as described in their paper (Donnat et al., 2018). The resulting representations are of dimension 100.

For GCC (Qiu et al., 2020), we used the model pretrained using MOCO available via the GCC Github repository <https://github.com/THUDM/GCC>¹. This model outputs representations of dimension $d = 64$.

The manual features, described in Section 3.1, use egonet radii $\rho \in \{1, 2, 3, 4\}$ and compute the following commonly used egonet graph statistics as features for each ρ : number of nodes, average and max node degree, number of triangles, global clustering coefficient (Newman, 2003a) and assortativity coefficient (Newman, 2003b). Thus, the resulting representations are of dimension 24.

B.2. Gradual Structure Perturbation

In this section, we provide detailed descriptions of the rewiring procedures used in the experiments in Section 4.2.

Configuration model. The configuration rewiring algorithm iterates through the edges in the graph and for each edge attempts to swap its target or source with the target or source of another edge in the graph such that the degrees of the involved nodes remain unchanged. This is repeated until a given fraction of the total number of edges has been rewired.

Rewiring subgraphs. Given an induced subgraph $H = (V_H, E_H)$ of a graph $G = (V_G, E_G)$ and a perturbation fraction $\eta \in [0, 1]$, the goal is to add or remove a total of $m_{\pm} = \lfloor \eta |E_H| \rfloor$ edges between nodes in the subgraph only without disconnecting the subgraph. Thus, a random minimum spanning tree of the subgraph containing $|V_H| - 1$ edges is first extracted. Thereafter, $m_- = \min(0.5m_{\pm}, |E_H| - (|V_H| - 1))$ randomly chosen edges not in the tree are removed, and an additional $m_+ = m_{\pm} - m_-$ randomly chosen edges, not present in the unperturbed subgraph, are added. This procedure

¹Specifically, the model specified as `Pretrain_moco_True_dgl_gin_layer_5_lr_0.005_decay_1e-05_bsz_32_hid_64_samples_2000_nce_t_0.07_nce_k_16384_rw_hops_256_restart_prob_0.8_aug_1st_ft_False_deg_16_pos_32_momentum_0.999` was used.

Table 3. Graph statistics for a graph $G = (V, E)$ with $N = |V|$ nodes. The table is extracted from (Bojchevski et al., 2018) and (Rendsburg et al., 2020).

STATISTIC NAME	COMPUTATION	DESCRIPTION
MAX DEGREE	$\max_{v \in V} d(v)$	Maximum degree of all nodes in a graph with $d(v)$ denoting the degree of node v .
ASSORTATIVITY	$\frac{\text{Cov}(X, Y)}{\sigma_X \sigma_Y}$	Pearson correlation of degrees of connected nodes where the (x_i, y_i) pairs are the degrees of connected nodes (Newman, 2003b).
GLOBAL CLUSTERING COEF.	$3 \times \frac{\text{Tr} \mathbf{A}^3}{\sum_{i \neq j} [\mathbf{A}^2]_{i,j}}$	The ratio of number of closed triplets to the total number of triplets. Measures the degree to which nodes in a graph tend to cluster together (Newman, 2003a).
POWER LAW EXPONENT	$1 + N \left(\sum_{v \in V} \log \frac{d(v)}{d_{\min}} \right)^{-1}$	Exponent of the power law distribution where d_{\min} denotes the minimum degree in the graph (Newman, 2018).
CHARACTERISTIC PATH LENGTH	$\frac{1}{N(N-1)} \sum_{u \neq v} d(u, v)$	Average shortest path length where $d(u, v)$ is the shortest path length between nodes u and v .

GraphDCA Framework for Node Distribution Comparison

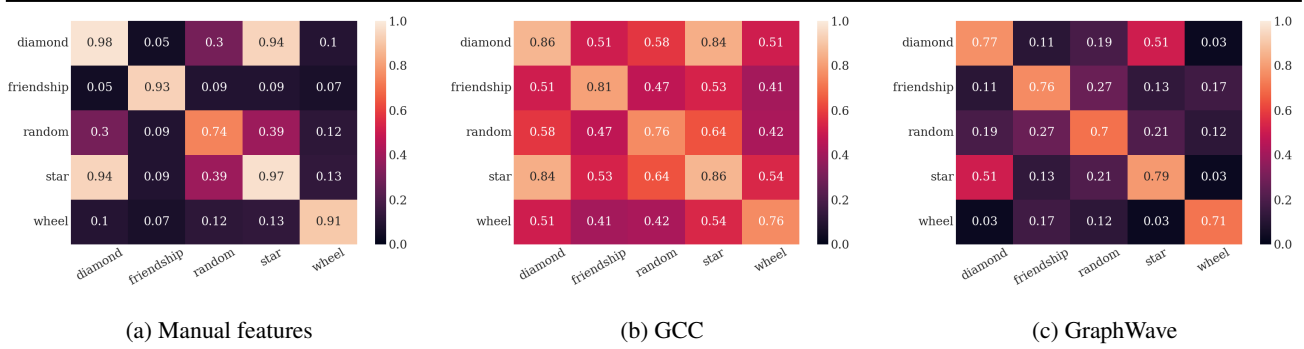


Figure 7. Matrices with values representing the average s_{wDCA} scores obtained for various feature extractors f and $G_1, G_2 \in \{G_h^{cycle} | h = diamond, friendship, random, star, wheel\}$. The result is averaged over 3 runs. Here, s_{wDCA} is calculated using uniform weights $w_i = 1$ for all nodes in G_1, G_2 .

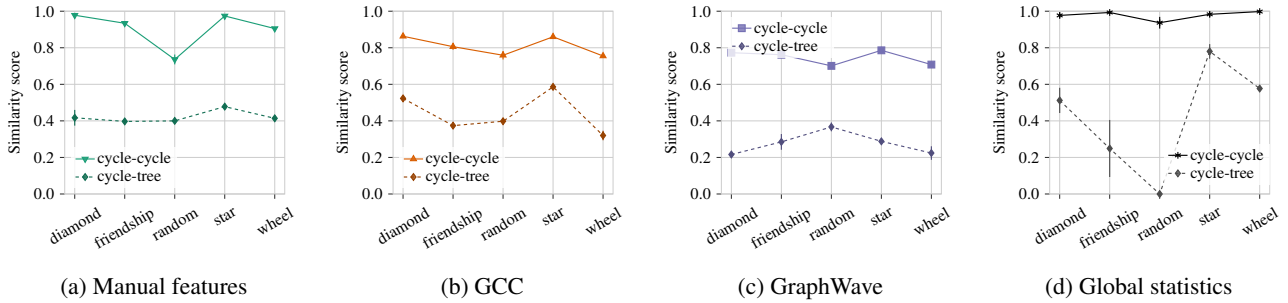


Figure 8. Average s_{wDCA} score ((a), (b), (c)) obtained between two input graphs with fixed type of subgraphs h having same main graph, i.e., $G_1 = G_h^{cycle}, G_2 = G_h^{cycle}$ (solid lines), and having different main graphs, i.e., $G_1 = G_h^{cycle}, G_2 = G_h^{tree}$ (dashed lines). The corresponding relative global statistics of input graphs $s_{gstats}(G_1, G_2)$ are shown in (d). The result is averaged over 3 runs. Here, s_{wDCA} is calculated using uniform weights $w_i = 1$ for all nodes in G_1, G_2 .

may fail for very dense subgraphs, specifically if the graph density exceeds 0.5, i.e. $|E_H| > 0.5 \binom{|V_H|}{2}$, as then a sufficient number of new edges cannot be added. However, no such subgraphs are part of the GROLETEST dataset and it is therefore ignored.

B.3. Generative Models Hyperparameters

NetGAN. We used the following default parameters for NetGAN recommended by the authors [Bojchevski et al. \(2018\)](#) or provided in their official Github repository: 3 discriminator iterations are performed per generator iteration, learning rate is set to 0.0003 with initial temperature of 5 and temperature decay 0.99998. Generator and discriminator weight matrix sizes were set to 32 and 128, L_2 penalty values to 10^{-7} and $5 \cdot 10^{-5}$, layer counts to 40 and 30, respectively. Training was performed with an edge overlap 0.5 stopping criterion, or with a validation score criterion stopped after 20 evaluations without improvement. Stopping criteria were evaluated every 2000 iterations. Random walk length during training and generation was set to 16. In total, 60,000 random walks with Gumbel-Softmax temperature parameter 0.5 were sampled to create an edge score matrix.

CELL. We used hyperparameters provided in the original publication ([Rendsburg et al., 2020](#)). Logit space rank (H) was set to 9, stopping criterion of 0.5 edge overlap was invoked every 10 iterations, otherwise the training was stopped after 300 iterations. Learning rate was set to 0.1 with weight decay 10^{-7} .

C. Additional Results

In this section, we report additional results supporting the discussions in the main paper. Specifically, we present the results of our experiments when using uniform weighting, $w_i = 1$ for all i , in the s_{wDCA} score.

C.1. Local Structural Similarity

In Figures 7 and 8 we show s_{wDCA} scores corresponding to the local structural similarity experiments, as described in Section 4.1, using uniform weighting. Comparing Figures 7 and 3, displaying the s_{wDCA} scores obtained for GROLETEST graphs with *cycle* main graph and varying subgraph types, we observe that off-diagonal elements are generally higher when using the uniform weighting. This is expected since the GROLETEST graphs in this experiment share the same main graph (*cycle*) and the similarity of the local structure of main graph nodes is reflected in the s_{wDCA} scores. We note that off-diagonal elements are particularly pronounced for GCC. We hypothesize that this could be an effect of the random walk subgraph sampling which results in more uniform distribution of node representations.

The opposite effect is observed for similarities calculated on GROLETEST graphs with different main graphs, shown in Figure 8. Since all nodes receive equal weight, the differences in the main graph structure are also accounted for which results in lower values for $s_{wDCA}(G_h^{cycle}, G_h^{tree})$ compared to values obtained with weighting of central nodes reported in Figure 4.

C.2. Gradual Structure Perturbation

In Figures 9a-9e, we report the results of the subgraph rewiring experiment, described in Section 4.2, using uniform weighting for the s_{wDCA} scores. Additionally, the rewiring results using the *random* subgraphs omitted from Figure 6 are shown in Figure 9f.

When using uniform weighting, the s_{wDCA} scores increase for all feature extractors and for all rewiring fractions compared to the scores obtained with central node weighting shown in Figure 6. This is expected since only the edges of the subgraphs are perturbed meaning that the graphs share the same main graph for which the local structural similarity is preserved.

C.3. Evaluation of Graph Generative Models

In Table 4, we report the global graph statistics and s_{wDCA} scores obtained on real-world datasets for NetGAN models trained with Val and EO stopping criteria. The results are on par with prior conclusions about higher efficiency of EO criterion in generating new graphs. We highlight that s_{wDCA} scores provide a more clear comparison between two models in cases where all global statistics are either both similar or both different from the training values (see for example CORA-ML).

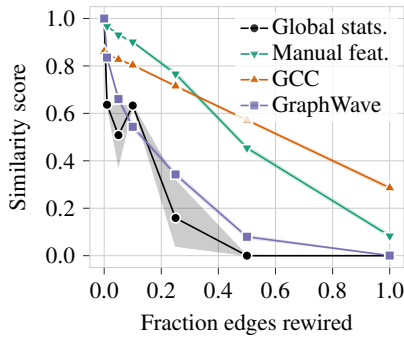
In Table 5, we report the global statistics and s_{wDCA} obtained on GROLETEST for subgraphs $h = random, star$. Similar to the results obtained for $h = diamond, friendship, wheel$ in Table 2, we observe that the models struggle to produce graphs that would well reflect all the global statistics with CELL being more efficient in replicating the egocentric networks among the two.

Table 4. Global graph statistics of the real-world training graphs G_1 and s_{DCA} scores obtained on representations extracted from the considered feature extractors f of G_1 and graphs G_2 generated by NetGAN trained with VAL and EO stopping criteria. The scores are averaged over 3 independently generated graphs with the same training split.

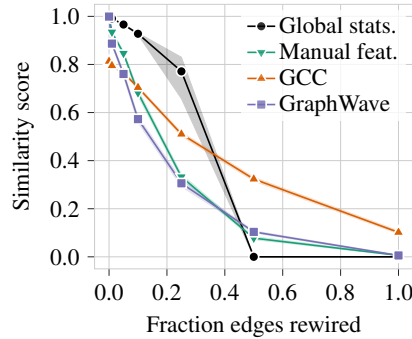
	CORA-ML			CITSEER			POLBLOGS		
	GROUND TRUTH	NETGAN VAL	NETGAN EO	GROUND TRUTH	NETGAN VAL	NETGAN EO	GROUND TRUTH	NETGAN VAL	NETGAN EO
MAX DEGREE	238	256.00 ± 10.82	216.00 ± 11.14	76	70.33 ± 12.22	88.00 ± 1.73	303	260.67 ± 5.13	279.33 ± 14.57
ASSORTATIVITY	-0.08	-0.04 ± 0.00	-0.08 ± 0.00	-0.19	-0.08 ± 0.00	-0.16 ± 0.00	-0.22	-0.25 ± 0.01	-0.25 ± 0.01
TRIANGLE COUNT	2,802	659.00 ± 28.36	1,772.33 ± 17.39	304	74.67 ± 11.59	195.33 ± 5.86	61,108	33,105.33 ± 360.05	36,294.33 ± 348.62
SQUARE COUNT	14,268	2,461 ± 7.81	6,741.33 ± 229.38	1,441	166.00 ± 17.44	371.33 ± 35.22	2,654,319	1,260,882.00 ± 7,415.16	1,350,075.67 ± 17,073.43
POWER LAW EXP.	1.86	1.78 ± 0.00	1.81 ± 0.00	2.45	2.28 ± 0.00	2.32 ± 0.01	1.44	1.40 ± 0.00	1.41 ± 0.00
CLUSTERING COEFF.	0.08	0.02 ± 0.00	0.06 ± 0.00	0.04	0.02 ± 0.00	0.03 ± 0.00	0.19	0.12 ± 0.00	0.13 ± 0.00
CHARC. PATH LEN.	5.63	4.80 ± 0.02	5.23 ± 0.03	8.02	6.00 ± 0.09	6.49 ± 0.20	2.82	2.64 ± 0.01	2.67 ± 0.00
$s_{wDCA} - \text{MANUAL}$	1.00	0.02 ± 0.01	0.11 ± 0.01	1.00	0.13 ± 0.01	0.22 ± 0.01	1.00	0.00 ± 0.00	0.00 ± 0.00
$s_{wDCA} - \text{GCC}$	0.73	0.23 ± 0.02	0.51 ± 0.00	0.75	0.35 ± 0.02	0.50 ± 0.01	0.66	0.34 ± 0.03	0.38 ± 0.02
$s_{wDCA} - \text{GRAPHWAVE}$	1.00	0.18 ± 0.01	0.52 ± 0.01	1.00	0.32 ± 0.01	0.53 ± 0.03	1.00	0.43 ± 0.02	0.50 ± 0.01

Table 5. Global graph statistics of GROLETEST *random* and *star* training graphs G_1 and s_{wDCA} scores obtained on representations extracted from the considered feature extractors f of G_1 and graphs G_2 generated by NetGAN and CELL (50% EO stopping criterion). The scores are averaged over 3 independently generated graphs with the same training split.

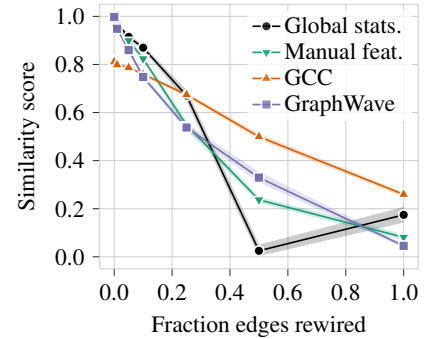
	RANDOM			STAR		
	GROUND TRUTH	NETGAN	CELL	GROUND TRUTH	NETGAN	CELL
MAX DEGREE	6	7.33 ± 1.53	8.00 ± 1.0	5	6.67 ± 0.58	6.33 ± 0.58
ASSORTATIVITY	-0.04	-0.14 ± 0.02	-0.02 ± 0.03	0.08	-0.14 ± 0.03	0.10 ± 0.01
TRIANGLE COUNT	0	103.67 ± 9.45	0.00 ± 0.00	0	107.33 ± 9.29	0.67 ± 0.58
SQUARE COUNT	0	46.00 ± 3.61	9.33 ± 0.58	0	46.67 ± 2.08	12.67 ± 2.08
POWER LAW EXP.	2.59	2.73 ± 0.01	2.70 ± 0.00	2.50	2.71 ± 0.01	2.65 ± 0.01
CLUSTERING COEFF.	0.00	0.11 ± 0.01	0.00 ± 0.00	0.00	0.12 ± 0.01	0.00 ± 0.00
CHARC. PATH LEN.	83.73	14.97 ± 0.75	17.85 ± 0.81	79.50	10.98 ± 3.16	18.84 ± 0.37
$s_{wDCA} - \text{MANUAL}$	1.00 ± 0.00	0.41 ± 0.03	0.73 ± 0.01	1.00 ± 0.00	0.32 ± 0.03	0.66 ± 0.02
$s_{wDCA} - \text{GCC}$	0.76 ± 0.02	0.49 ± 0.02	0.70 ± 0.00	0.80 ± 0.02	0.33 ± 0.03	0.62 ± 0.02
$s_{wDCA} - \text{GRAPHWAVE}$	1.00 ± 0.00	0.32 ± 0.00	0.47 ± 0.02	1.00 ± 0.00	0.11 ± 0.01	0.26 ± 0.02



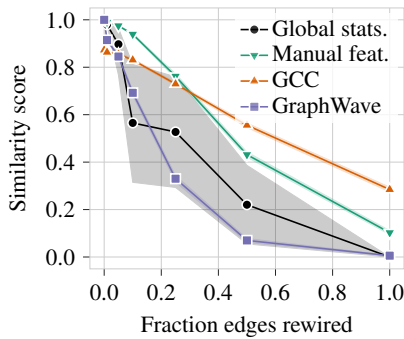
(a) Diamond



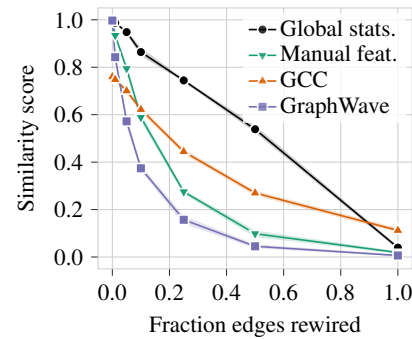
(b) Friendship



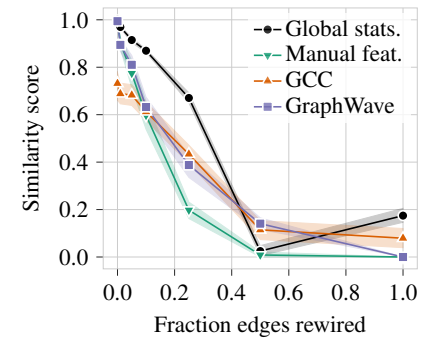
(c) Random



(d) Star



(e) Wheel



(f) Random with node importance weighting

Figure 9. Rewiring of GROLETEST subgraphs via the addition and removal of edges. The x-axis specifies the fraction of changed edges. The y-axis shows s_{gstats} scores (in black) and s_{wDCA} scores for three different feature extractors (in color), averaged over 5 different rewirings. For Figures (a)-(e), s_{wDCA} is calculated using uniform weights $w_i = 1$ for all nodes. In Figure (f), the s_{wDCA} score is calculated using weighting of the central nodes where $w_i = 0$ for all nodes except for the 20 central nodes in the subgraphs which receive $w_i = 1$ (see also Figure 6).